Letters

An Enhanced DC Preexcitation With Effective Flux-Linkage Control for the High-Power Induction Motor Drive System

Sideng Hu, Zhengming Zhao, Hua Bai, and Liqiang Yuan

***Abstract*—This paper proposed an enhanced dc preexcitation for a variable-voltage variable-frequency-controlled induction motor drive system. Voltage vectors were adjusted according to the reactive component of the motor current, which promptly established the effective value of the motor flux linkage at the preexcitation stage and restrained its trajectory strictly as a round circle all through the starting process. The enhanced dc preexcitation control led to more negligible flux-linkage distortion, less torque vibration, and significantly smaller inrush current. Experiments on a 380-VAC/315-kW adjustable speed drive system validated the effectiveness of the proposed method.**

***Index Terms*—Adjustable speed drive (ASD) system, dc preexcitation, induction motor (IM), startup, variable-voltage variable frequency (VVVF).**

I. Introduction

In motor drive systems, the startup control is always a critical issue due to the inrush current in the starting process, which tends to damage the motor insulation and endanger the semiconductor devices [1]–[4]. It is highly related to the absence of the effective flux linkage. Vector controls, e.g., the direct torque control (DTC) and field-oriented control (FOC), have been validated capable of delivering the targeted torque and depressing the startup current through processing the accurate flux-linkage observation and control. However, they suffer from the nonlinearity of power devices and the complication of the parameter identification. Both FOC and DTC face the challenges of the inaccurate flux-linkage observation, which is of particular importance for the sensorless vector control at low-speed operation [5], [6].

One feasible solution is to adopt the variable-voltage variable-frequency (VVVF) control in the starting process and smoothly switch to the sensorless vector control in the high-speed region [7]–[9]. In the previous study [10]–[12], a dc preexcitation control in a three-level VVVF-controlled induction motor (IM) drive system was proposed, which establishes the initial back electromotive force (EMF) before the motor gets started. Therefore, it effectively depressed the inrush current and increased the starting torque. However, its effect will be discounted by the absence of flux-linkage control in the whole starting process. This will lead to the flux-linkage distortion, thereby, the overcurrent and insufficient torque.

As an extension of the previous study on the dc preexcitation [10], this paper will analyze its disadvantages, enhance the dc preexcitation with one simple and effective flux-linkage controller, and validate its effectiveness through simulations and experiments in a two-level three-phase 380-VAC/315-kW motor drive system. Different startup strategies will also be detailed through experiments.

Manuscript received October 17, 2010; revised January 18, 2011; accepted March 6, 2011. Date of current version September 16, 2011. This work was supported by the key program of the National Natural Science Foundation of China under Grant 50737002 and Grant 50707015. Recommended for publication by Associate Editor J. Biela.

S. D. Hu, Z. M. Zhao, and L.Q. Yuan are with the Department of Electrical Engineering, Tsinghua University, Beijing 100084, China (e-mail: hsd06@mails.tsinghua.edu.cn; zhaozm@mail.tsinghua.edu.cn; ylq@tsinghua.edu.cn).

H. Bai is with the Department of Electrical and Computer Engineering, Kettering University, Flint, MI 48504 USA (e-mail: hbai@kettering.edu).

Digital Object Identifier 10.1109/TPEL.2011.2131680

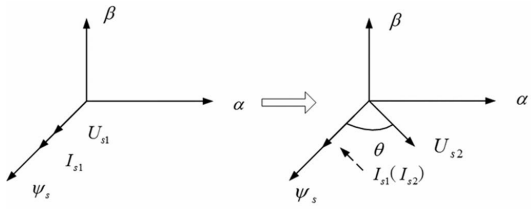

Fig. 1. Vector scheme in the motor start moment: (a) before startup and (b) at the startup moment, I_{s1} and I_{s2} could be viewed as equal.

II. Principles of the DC Preexcitation and its Demerits

DC preexcitation establishes the flux linkage of the IM through imposing a dc current on the motor before it starts up. The stator flux linkage can be expressed as follows:

$$\psi_s = L_s \cdot I_s + L_m \cdot I_r \tag{1}$$

where I_s is the stator current, I_r is rotor current, L_s is the stator leakage inductance, and L_m will be the excitation inductance. In the dc preexcitation, I_r is close to zero. In this case, stator flux linkage can be simplified as follows:

$$\psi_s = L_s \cdot I_s. \tag{2}$$

Fig. 1 shows the voltage vectors at the moment when the dc preexcitation process is switched to the starting process. I_{s1} is the preexcitation current and I_{s2} is the current at the startup moment. As mentioned in [10], I_{s1} and I_{s2} could be viewed as equal at this moment, and the slope of the flux linkage is

$$\frac{d}{dt}\psi_s = \frac{\psi_s(t_s + \Delta t) - \psi_s(t_s)}{\Delta t} = U_{s2} - I_{s1} * R_s \tag{3}$$

where U_{s2} is stator voltage vector in startup process, and R_s is the stator resistance. By cross multiplying I_{s2} at both sides of equation (3),we get

$$\frac{\psi_s(t_s+\Delta t)\otimes I_{s2}-\psi_s(t_s)\otimes I_{s2}}{\Delta t}=U_{s2}\otimes I_{s2}. \quad (4)$$

Since the electromagnetic torque is

$$T_e=p_n(\psi_s\otimes i_s) \quad (5)$$

therefore

$$\left|\frac{dTe}{dt}\right|\approx p_n\left|U_{s2}\otimes I_{s2}\right| \quad (6)$$

where p_n is the pole number in the motor.

Equation (6) is the essence of the previously proposed dc preexcitation, which implies that at the starting moment, a voltage vector U_{s2} perpendicular to the excitation current vector I_{s1} will maximize the torque. Also, the established flux linkage will induce back EMF to effectively restrain the inrush current.

However, (6) can only hold voltage vector perpendicular to excitation current for the first several switching periods during the starting process. When the motor begins rotating, the angle between the voltage vector and the excitation current I_{s1}cannot be guaranteed as direct angle. Therefore, (6) is no longer satisfied, which degrades the effect of the dc preexcitation. This also leads to atrocious amount of effort to get the optimal preexcitation current value, direction, and time, as shown in [10].

Equation (5) can be written as follows:

$$\frac{dTe}{dt}=p_n\left(\frac{d\psi_s}{dt}\otimes I_{s2}+\psi_s\otimes\frac{dI_{s2}}{dt}\right). \quad (7)$$

Since $d\psi_s/dt=U_s-I_sR_s$, (7) could be derived as follows:

$$\frac{dTe}{dt}=p_n\left((U_{s2}-I_{s2}\cdot R_S)\otimes I_{s2}+\psi_s\otimes\frac{dI_{s2}}{dt}\right). \quad (8)$$

In the *d–q* coordinate axis, (8) could be expressed as follows:

$$\frac{dT_e}{dt}=p_n\left(U_s\otimes(I_{sd}+jI_{sq})+\psi_s\otimes\frac{d(I_{sd}+jI_{sq})}{dt}\right). \quad (9)$$

Note here that I_{sd} is the current mapped along the U_s, and I_{sq} is kept vertical to U_s, which is totally different from the traditional *d–q* transformation in FOC. A constant I_{sq} will result in $dI_{sq}/dt=0$. Therefore,

$$\frac{dT_e}{dt}=p_n\left(U_sI_{sq}+\psi_s\otimes\frac{dI_{sd}}{dt}\right). \quad (10)$$

Moreover, digitizing (10) leads to

$$\Delta T=p_n(U_sI_{sq}\Delta t+\Psi_s\otimes\Delta I_{sd}). \quad (11)$$

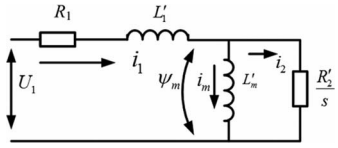

Fig. 2. Equivalent circuit diagram for IM.

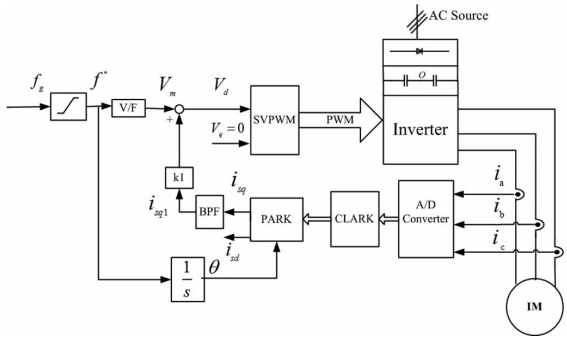

Fig. 3. Diagram of the proposed method.

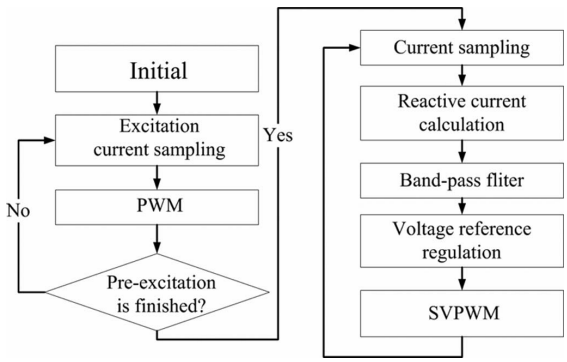

Fig. 4. Flow chart of the proposed method.

Equation (11) extends the effective area of the dc preexcitation to the whole startup process. Equation (6) is only an exception assuming that $dI_{sd}/dt=0$.

III. Enhanced DC Preexcitation

As it was pointed in Section II, $dI_{sq}/dt=0$ is the precondition of (11). However, different from FOC and DTC, the conventional VVVF control is a typical open-loop control without any current decoupling. Here, we need first derived the expression of i_{sd} and i_{sq} based on the equivalent circuit of an IM, as shown in Fig. 2.

I_{sd} and I_{sq} represent the active and reactive current in Fig. 2, respectively, which are expressed as follows, as shown (12) and (13), at the bottom of next page page.

$$I_{sd}=\frac{\left(R_1R'^2_2+\omega^2L'^2_ms^2R_1+\omega^2L'^2_msR'_2\right)U_1}{\omega^4L'^2_1L'^2_ms^2+\left((R_1s+R'_2)^2L'^2_m+2L'_1R'^2_2L'_m+L'^2_1R'^2_2\right)\omega^2+R_1^2R'^2_2} \quad (12)$$

$$I_{sq}=-\frac{\left(\omega L'_1R'^2_2+R'^2_2\omega L'_m+\omega^3L'^2_ms^2L'_1\right)U_1}{\omega^4L'^2_1L'^2_ms^2+\left((R_1s+R'_2)^2L'^2_m+2L'_1R'^2_2L'_m+L'^2_1R'^2_2\right)\omega^2+R_1^2R'^2_2}. \quad (13)$$

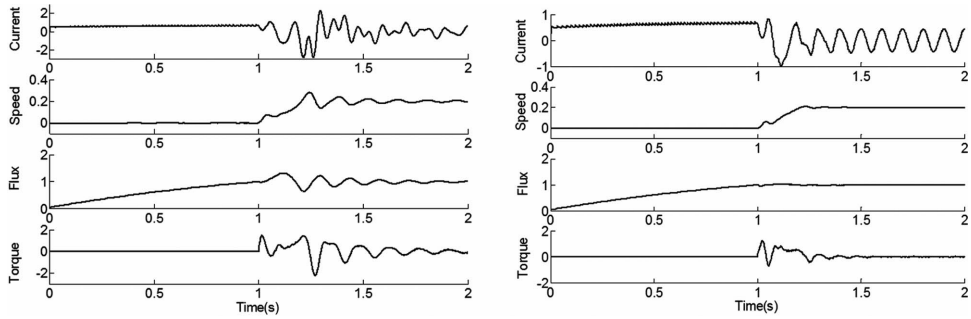

Fig. 5. Comparison of the starting processes (simulations). (a) Traditional preexcitation method and (b) Proposed method.

TABLE I
KEY PARAMETERS FOR THE ASD SYSTEM

parameter	value
rated power (motor)	315kW
rated voltage (motor)	380VAC
rated current (motor)	545A
dead time of IGBTs	3μs
switching frequency in pre-excitation	1.6kHz
switching frequency in motor start-up	3.2kHz
minimum pulse width	2.4/μs
maximum pre-excitation current	473(0.7pu)A

When motor begins to start, s tends to be a small value. L'_1, R_1, and R_2 are all negligible compared to $\omega L'_m$. A simplified expression of I_{sq} can be written as follows:

$$I_{sq} \approx -\frac{\left(R'^2_2 \omega L'_m\right) U_1}{\left(R'^2_2 L'^2_m\right) \omega^2} = -\frac{U_1}{\left(L'_m\right) \omega} = -\frac{\psi_s}{L'_m}. \tag{14}$$

It is pointed out by (14) that the flux-linkage distortion roots in the uncontrolled I_{sq}. Physically, it could be explained as: increased I_{sq} amplitude indicates the increased flux linkage. It needs to noticed the negative sign in (14) for implementation.

In the first step, I_{sq} is obtained by transforming the three-phase stator currents into two perpendicular components through the park transformation [13]. Since θ, the angle of the voltage vector, is known from the VVVF control, the reactive and active currents can be calculated as follows:

$$\begin{bmatrix} I_\alpha \\ I_\beta \end{bmatrix} = \begin{bmatrix} 1 & -\frac{1}{2} & -\frac{1}{2} \\ 0 & \frac{\sqrt{3}}{2} & -\frac{\sqrt{3}}{2} \end{bmatrix} \begin{bmatrix} I_a \\ I_b \\ I_c \end{bmatrix}$$
$$\begin{bmatrix} I_{sd} \\ I_{sq} \end{bmatrix} = \begin{bmatrix} \cos\theta & \sin\theta \\ -\sin\theta & \cos\theta \end{bmatrix} \begin{bmatrix} I_\alpha \\ I_\beta \end{bmatrix} \tag{15}$$

where I_a, I_b, and I_c are three-phase stator currents, I_α and I_β are the α- and β-axis components in the α–β coordinates, respectively, and θ is the angle of the voltage vector.

In order to obtain the fundamental current, a bandpass filter is used, whose upper cutoff frequency is lower than the switching frequency, and lower cutoff frequency is close to 0 Hz because the reactive current is supposed to be a dc signal. Here, 100 and 5 Hz are chosen for each of the frequencies, respectively.

The whole control scheme is shown as Fig. 3. I_{sq} is transformed into a voltage value through a gain amplifier and added

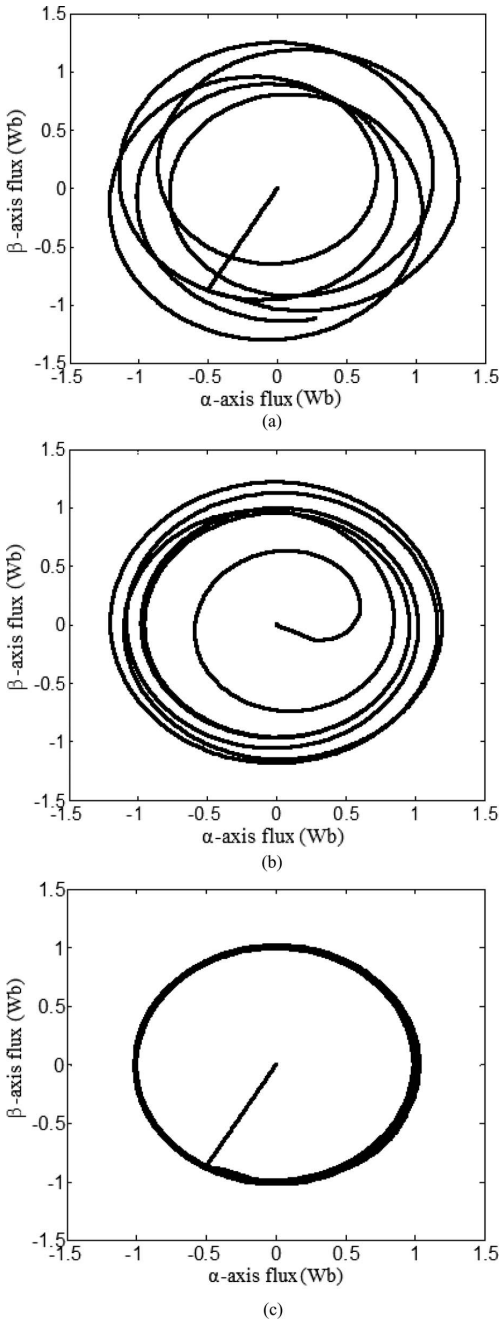

Fig. 6. Stator flux linkage in three startup methods: (a) with flux-linkage control method only, (b) with dc preexcitation only, and (c) with both (a) and (b).

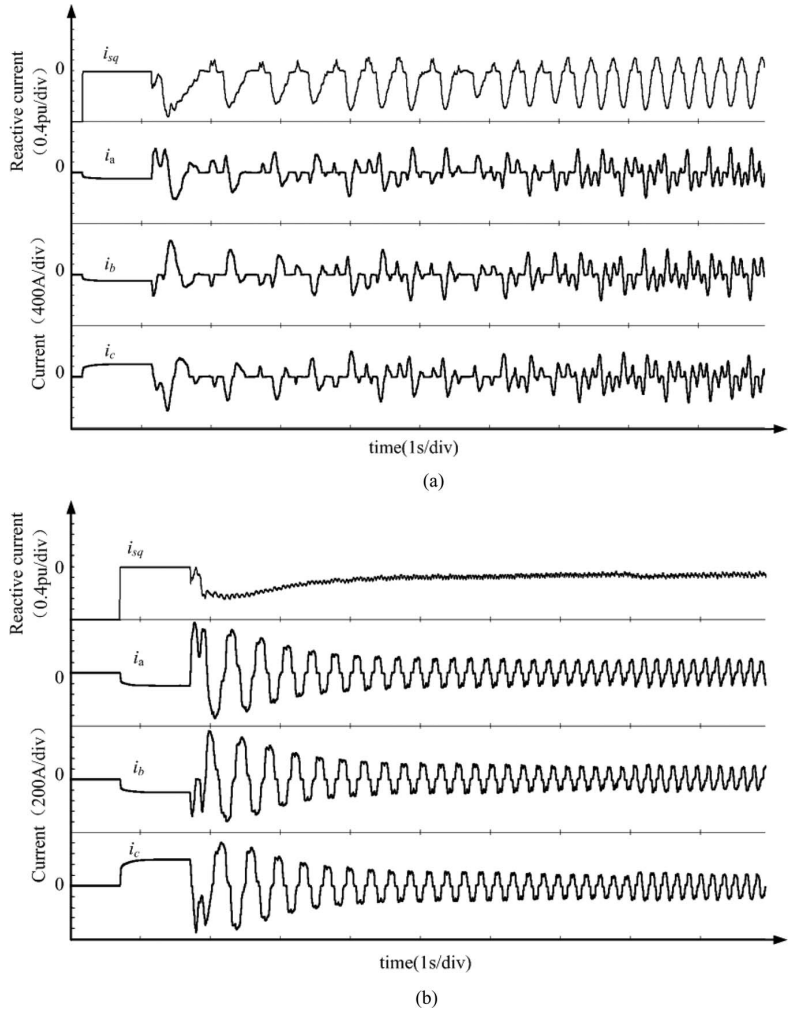

Fig. 7. Comparison of the reactive current in the starting process (experiments). (a) Traditional preexcitation method and (b) proposed method.

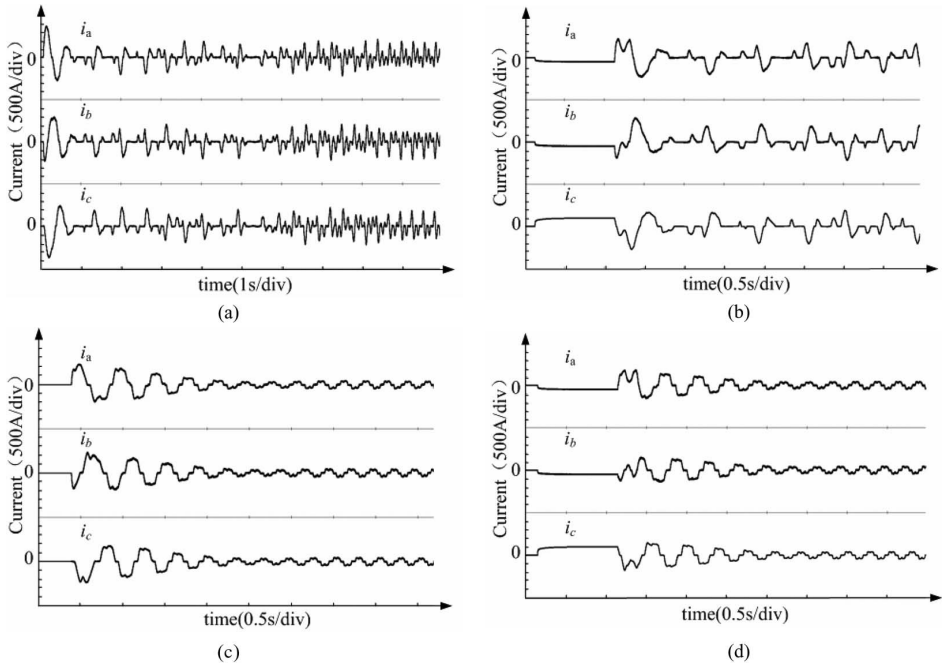

Fig. 8. Experimental comparison of four startup methods: (a) direct startup, (b) startup with preexcitation, (c) startup with flux control method, and (d) startup with proposed method.

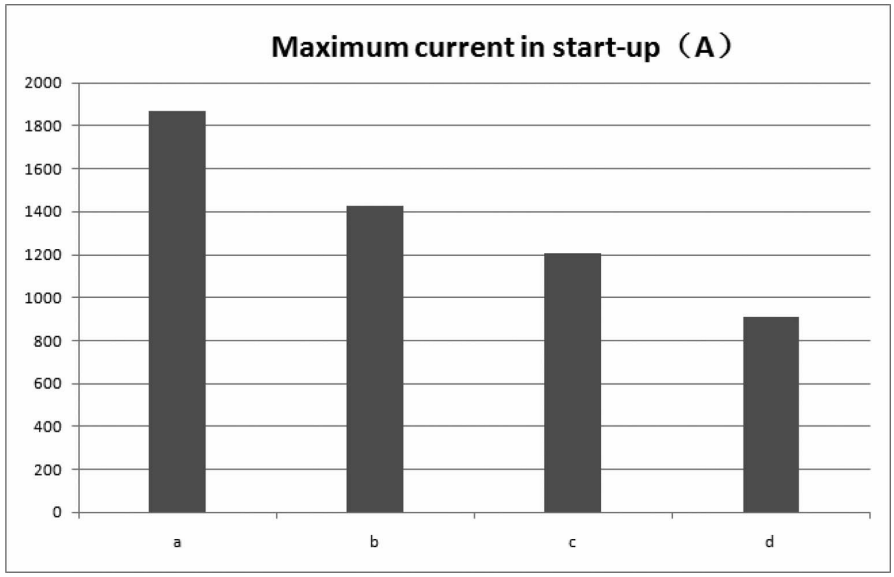

Fig. 9. Maximum current of four startup methods (experiments): (a) direct startup, (b) startup with preexcitation, (c) startup with flux control method, and (d) startup with the proposed method.

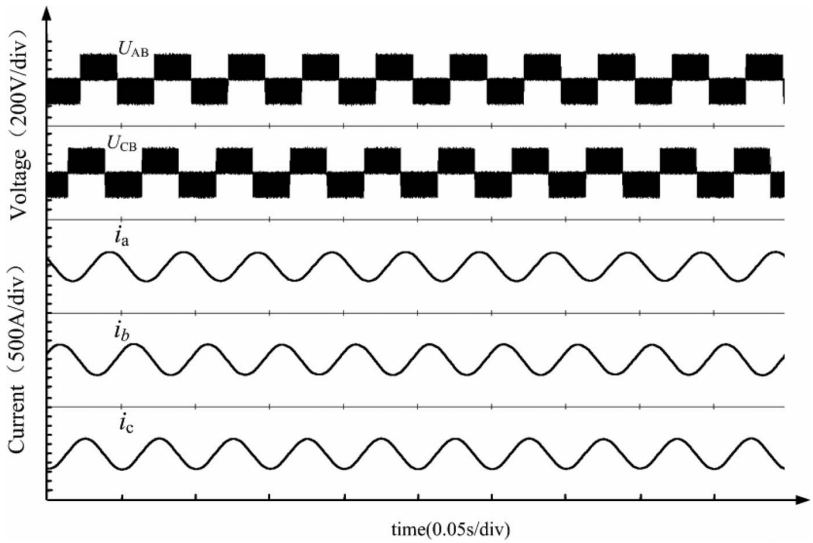

Fig. 10. Full-load experiment in 20 Hz (experiment).

to the voltage reference V_m generated by the VVVF algorithm. Negative sign in (14) indicate that the amplitude of the voltage vector V_d should be decreased according to the increased amplitude of I_{sq}; therefore, k_1 is positive. The dynamic effect of depressing the reactive-current fluctuation and thereby the flux-linkage fluctuation will improve as k_1 increases. However, it should not overcompensate in case the system gets unstable.

IV. Simulation and Experiment Results

The effectiveness of the proposed start strategy for the IM drive system is validated by simulations and experiments, whose flow chart is shown as Fig. 4.

A comparison between the traditional preexcitation method and proposed method has been carried out by numerical simulations in Fig. 5(a) and (b). The proposed method has obvious effect on dampening the vibration in current, speed, flux, and torque by the proposed method. Fig. 6 shows the simulation result of the flux linkage locus in three different startup methods. It can be seen in Fig. 6(a) that the flux is gradually established. Fig. 6(b) established the flux linkage promptly; however, when the motor starts, the flux linkage tends to oscillate. In Fig. 6(c), dc preexcitation helps establish the flux initial value at the startup moment, and another controller helps restrain the flux linkage as a round locus. Therefore, the dynamic process of building flux linkage is shortened compared to (a) and (b), which results in a smaller in-rush current, less torque oscillation, and faster convergence.

The proposed method is tested by experiments in a 380-V/315-kW adjustable speed drive (ASD) system, whose electrical ratings are reported in Table I. Here, four insulated gate bipolar transistors (IGBTs) are paralleled together, which

totally can handle 2000 A. Fig. 7 shows the experimental comparison between the conventional dc preexcitation and the proposed method. Fig. 7(a) indicates the traditional dc preexcitation process. In Fig. 7(b), the fluctuation of the reactive current I_{sq} is effectively depressed; therefore, the starting process is significantly improved, which is consistent with the analysis in Section III.

Fig. 8 shows the comparison of four startup strategies under the same VVVF startup condition with no load. The four methods are: 1) directly startup, 2) startup with preexcitation only, 3) startup with flux-linkage control method only, and 4) startup with the proposed method. In Fig. 8(a) and (b), the inrush current larger than 1800 and 1400 A occurs in startup process, respectively. In Fig. 8(c), the maximum in-rush current is 1200 A. In Fig. 8(d), the peak value of current is less than 900 A. More specifically, the maximum currents of four startup strategies under the same VVVF startup condition are compared in Fig. 9. The proposed startup method helps shrink 950 A in the starting process, while only 400 A is saved with conventional dc preexcitation control. Due to the improvement in the starting process, eventually only three IGBTs (450 A) in parallel are needed, which significantly saves the cost of the ASD system.

Fig. 10 shows the full-load experiment in 20 Hz, which demonstrated that the proposed method also works well in the full-load steady-state operation.

V. Conclusion

DC preexcitation is one of the effective solutions to increase the starting torque and depress the starting inrush current in a VVVF-controlled IM ASD system. The conventional dc preexcitation suffers from the flux distortion, therefore, its effect gets discounted after the first few switching periods. This paper analyzed the demerits of the conventional dc preexcitation method, and proposed an enhanced dc preexcitation by deploying an effective and simple flux-linkage controller. The initial value of the flux linkage is built by the previously proposed dc preexcitation, and its trajectory is kept as a round locus during the whole starting process. As an extension of dc preexcitation in [10], the proposed method has been validated more capable of depressing the torque vibration and inrush current.

This method is especially suitable for the high-power application. No parameter identifications, no speed coder, and no effort to seek the optimal preexcitation current are needed. It is also worthwhile to point out that the proposed method may also be applied in different voltage source inverters, including multilevel ASD systems.

References

[1] T. Quang-Vinh, C. Tae-Won, L. Hong-Hee, K. Heung-Geun, and N. Eui-Cheol, "Simple starting-up method of BLDC sensorless control system for vehicle fuel pump," in *Proc. IEEE Int. Power Electron. Conf.*, Jun. 2010, 2011, pp. 2244–2248.

[2] G. H. Jang, J. H. Park, and J. H. Chang, "Position detection and start-up algorithm of a rotor in a sensorless BLDC motor utilizing inductance variation," in *Proc. IEE Electric Power Appl.*, Mar. 2002, vol. 149, no. 2, pp. 137–142.

[3] W. J. Lee and S. K. Sul, "A new starting method of BLDC motors without position sensor," *IEEE Trans. Ind. Appl.*, vol. 42, no. 6, pp. 1532–1538, Nov./Dec. 2006.

[4] G. Juhasz, S. Halasz, and K. Veszpremi, "New aspects of a direct torque controlled induction motor drive," in *Proc. IEEE Int. Conf. Ind. Technol. Conf.*, Jan. 2000, pp. 43–48.

[5] J. Holtz, "Sensorless control of induction machines—With or without signal injection?," *IEEE Trans. Ind. Electron.*, vol. 53, no. 1, pp. 7–30, Feb. 2005.

[6] Y. S. Jeong, R. D. Lorenz, T. M. Jahns, and S. K. Sul, "Initial rotor position estimation of an interior permanent-magnet synchronous machine using carrier-frequency injection method," *IEEE Trans. Ind. Appl.*, vol. 41, no. 1, pp. 38–45, Jan./Feb. 2005.

[7] D. Jiang, R. X. Lai, F. Wang, R. Burgos, and D. Boroyevich, "Start-up transient improvement for sensorless control approach of PM motor," in *Proc. IEEE Appl. Power Electron. Conf.*, Feb. 2010, pp. 408–413.

[8] R. P. Burgos, P. Kshirsagar, A. Lidozzi, F. Wang, and D. Boroyevich, "Mathematical model and control design for sensorless vector control of permanent magnet synchronous machines," in *Proc. IEEE Workshop Comput. Power Electron. Conf.*, Jul. 2006, pp. 76–82.

[9] F. Parasilit, R. Petrella, and M. Tursini, "Sensorless speed control of a PM synchronous motor by sliding mode observer," in *Proc. IEEE Int. Symp. Ind. Electron. Conf.*, Jul. 1997, pp. 1106–1111.

[10] H. Bai, Z. M. Zhao, L. Q. Yuan, and B. Li, "A high voltage and high power adjustable speed drive system using the integrated LC and step-up transforming filter," *IEEE Trans. Power Electron.*, vol. 21, no. 5, pp. 1336–1346, Sep. 2006.

[11] S. D. Hu, Z. M. Zhao, T. Lu, and L. Q. Yuan, "DC pre-excitation application in three-phase induction motor drive system," in *Proc. IEEE Int. Symp. Power Electron. Distrib. Generation Syst.*, Jun. 2010, pp. 389–393.

[12] S. D. Hu, Z. M. Zhao, T. Lu, and L. Q. Yuan, "Approaches to enhance discrete control algorithms serving for motor drive system," in *Proc. IEEE Energy Convers. Congr. Expo.*, Sep. 2010, pp. 1041–1046.

[13] W. Chen, R. F. Yang, Y. Yu, G. L. Wang, and D. G. Xu, "A novel stability improvement method for V/F controlled induction motor drive systems," in *Proc. Int. Conf. Electr. Mach. Syst.*, Oct. 2008, pp. 1073–1076.